ELSEVIER

International Journal of Mass Spectrometry 204 (2001) 233–245

International Journal of Mass Spectrometry

Structure and reactivity of the prototype iron–oxide cluster $Fe_2O_2^+$

Phillip Jackson[a], Jeremy N. Harvey[b], Detlef Schröder[b,*], Helmut Schwarz[b]

[a]*Research School of Chemistry, Australian National University, Canberra ACT 0200, Australia*
[b]*Institut für Organische Chemie, Technische Universität Berlin, 10623 Berlin, Germany*

Received 8 March 2000; accepted 26 April 2000

Abstract

The iron–oxide cluster $Fe_2O_2^+$ is synthesized in the gas phase from a mixture of $Fe(CO)_5$ and O_2, and its gas-phase reactivity is subsequently probed using sector-field and Fourier-transform mass spectrometers. The experimental findings are in accord with, but do not establish that $Fe_2O_2^+$ has a rhombic structure with two equivalently bound oxo-ligands. Although the reactivity studies conducted with $Fe_2O_2^+$ are by and large consistent with previous literature data and the few thermochemical data available for ligated iron clusters, a severe discrepancy exists for the $Fe_2O_2^+/C_2H_4$ couple. Although exclusive dehydrogenation to afford $Fe_2C_2H_2O_2^+$ has been reported in a previous work [Gehret and Irion, Chem. Eur. J. 2 (1996) 598], this product constitutes a very minor channel in the present study; instead, various C–H and C–C bond activation processes as well as O-atom transfer from $Fe_2O_2^+$ to ethene are observed. A possible explanation is that two isomers and/or states of $Fe_2O_2^+$ cation were probed in the different experiments, thereby highlighting an important structural ambiguity in reactivity studies of transition-metal clusters. Assuming that the most stable $Fe_2O_2^+$ species is monitored in the present experiments, the reactions observed in combination with complementary thermochemical information imply heats of formation of $\Delta_f H_0(Fe_2O_2^-) = -32 \pm 12$ kcal/mol, $\Delta_f H_0(Fe_2O_2) = 22 \pm 12$ kcal/mol, and $\Delta_f H_0(Fe_2O_2^+) = 216 \pm 9$ kcal/mol for anionic, neutral, and cationic di-iron dioxide. (Int J Mass Spectrom 204 (2001) 233–245) © 2001 Elsevier Science B.V.

Keywords: Bond activation; FTICR-MS; Iron oxide; Metal–oxide clusters; Thermochemistry

1. Introduction

In a continuation of studies dealing with the chemistry of mononuclear metal–oxide ions [1,2], the gas-phase ion chemistry of transition-metal–oxide clusters keeps receiving increasing interest. Among the transition metals, in numerous respects, iron is certainly outstanding, and the possible implications of iron–oxide clusters range from fundamental properties to metallo-enzymes, surface catalysis, and corrosion phenomena. Here, we report mass spectrometric studies of the seemingly simple di-iron dioxide cation $Fe_2O_2^+$ as monitored under ion cyclotron resonance (ICR) conditions in conjunction with complementary experiments employing sector-field mass spectrometry.

In this study, we employ a chemical route for the generation of the $Fe_2O_2^+$ ion in the gas phase [3–5], whereas most of the previous reactivity studies employed sputtering methods [6–9]. As will be shown further, the ion's reactivity may depend upon the

* Corresponding author. E-mail: df@www.chem.tu-berlin.de

PII S1387-3806(00)00361-4

method of ion generation, indicating the existence of structural and/or electronic isomers.

Several recent studies pertaining to neutral and/or charged $Fe_2O_2^{+/0/-}$ species have been reported. Matrix-isolation experiments by Andrews and co-workers have provided vibrational frequencies of two isomers of neutral Fe_2O_2, a rhombic species and another, apparently linear form with an OFeFeO structure [10]. Wang and co-workers have determined an electron affinity $EA(Fe_2O_2) = 2.36$ eV using anion photoelectron spectroscopy [11]. Preliminary reactivity studies by Gehret and Irion have addressed the ion–molecule reactions of $Fe_2O_2^+$ with ethene, benzene, and ammonia [8]. Concerning the sequential Fe–O bond strengths in $Fe_mO_n^+$ clusters with $n = 1$ and 2, there existed some ambiguity, and it was assumed that $D_0(Fe_mO^+–O) \approx D_0(Fe_n^+–O)$ [4,8]. Detailed studies of Griffin and Armentrout have contributed valuable thermodynamic data for iron–oxide clusters of various sizes and confirmed this assumption for most $Fe_mO_n^+$ clusters except $m = 2$, however, these authors reported bond-dissociation energies $D_0(Fe_2O^+–O) = 99.2 \pm 7.7$ kcal/mol [12] and $D_0(Fe_2^+–O) = 117.6 \pm 4.6$ kcal/mol [13]. Finally, Cao et al. have performed an extensive theoretical analysis of neutral Fe_2O_2 [14].

The present study aims to extend the pioneering work of Gehret and Irion [8] by means of more detailed reactivity studies, bracketing and isotope exchange experiments using the ICR technique, complemented with a characterization of the $Fe_2O_2^+$ cation by means of sector-field mass spectrometry.

2. Experimental

Ion/molecule reactions are examined with a Spectrospin CMS 47X FTICR-MS equipped with an external ion source [15,16]. The $Fe_2O_2^+$ cluster is made by means of a gas-phase synthesis starting from bare Fe^+ stored in the ICR cell as described previously [4]. In brief, Fe^+ is generated by laser ablation of a solid steel sample using a Nd:YAG laser operating at 1064 nm. The ions are transferred to the ICR cell using a series of potentials and ion lenses. The cell itself is positioned in the bore of a 7.0 T superconducting magnet. In the ICR cell, mass-selected $^{56}Fe^+$ is then reacted with $Fe(CO)_5$ and O_2 introduced by way of pulse valves (up to 10^{-5} mbar maximum for 0.1 s). The trapped ions undergo more than 100 collisions, both reactive and nonreactive, during the time the pulse gas is in the ICR cell. After a typical delay of 3–4 s, most of the residual gases are pumped away, leaving behind a series of cationic iron–carbonyl, –oxocarbonyl, and –oxo clusters. The FERETS protocol [17] is then employed to mass select $Fe_2O_2^+$ for further reactions. Neutral reactants are introduced by means of leak valves to pressures of the order from 8×10^{-9} mbar to 1×10^{-7} mbar. The adjustment of the neutral's pressure depends on its reactivity towards key intermediates involved in the gas-phase synthesis of $Fe_2O_2^+$. For example, pressures up to 10^{-7} mbar of the less reactive reagents such as H_2, N_2, CO, and CO_2 can be admitted without seriously affecting the $Fe_2O_2^+$ yields. On the other hand, lower background pressures of, for example, C_2H_4 and NH_3 are necessary to prevent ion losses during the pumping delay that is required to remove the gases pulsed into the ICR cell during the synthesis of $Fe_2O_2^+$. All experimental second-order rate constants are evaluated assuming the pseudo-first-order kinetic approximation after calibration of the measured pressure and acknowledgement of the ion gauge sensitivities; the ion temperature is assumed as 298 K [18].

The neutral reagents, including $[D_4]$–ethene (Cambridge Isotope Laboratories, Andover, MA, USA) and $^{18}O_2$ (Campro Scientific, Emden, Germany), are used as purchased without further purification except for additional freeze–pump–thaw cycles.

Additional experiments were performed with a modified VG/ZAB/HF/AMD 604 four-sector mass spectrometer with BEBE configuration, where B represents magnetic and E electrostatic sectors, respectively [19]. The clusters were generated in a chemical ionization (CI) source by the electron bombardment (100 eV) of $Fe(CO)_5$ and O_2 [5]. For $Fe_2O_2^+$ interference by the isobaric ion $Fe(CO)_2O_2^+$ is negligible in the present study as no loss of CO ($\Delta m = 28$) is observed; see [5] for a discussion. All ions, accelerated to a nominal translational energy of 8 kV, are

mass-selected using B(1)E(1) prior to collision events. Two collision cells are positioned in the field-free region between E(2) and B(2), and the collision-gas pressures are maintained such that 80% of the parent ion beam is recovered after traversing a cell. In the average, this corresponds to approximately 1.0–1.5 collisions per ion [20]. B(2) is subsequently used to record the mass spectra in which 10–50 scans are averaged. Collisional activation (CA) is effected by colliding mass-selected $Fe_2O_2^+$ with oxygen, neutralization–reionization (NR) [21] experiments employ Xe and O_2 as collision gases for neutralization and reionization, respectively, and in charge reversal (CR) [22] of anions to cations oxygen is used as a collision gas. A deflector electrode positioned between the collision cells and maintained at 1 kV ensures no ions are transmitted to the second cell during the NR experiments, and only neutral species stable for approximately 1 μs may be recovered. The energy-resolved CR experiments are performed with B(1)-only mass-selected ions using the process $O_2^{-\cdot} \rightarrow O_2^{+\cdot}$ for calibration of the energy scale [23,24]; a definition of the ions' effective temperature is not indicated in these vertical transitions.

3. Results and discussion

3.1. Structure(s) and energetics of $Fe_2O_2^+$

On a general note and for specific reasons which become obvious further on, first, it is necessary to deal with the possible structures of the $Fe_2O_2^+$ cation in some more detail. Thus, already for mononuclear [M, O_2] species several structural isomers need to be considered, i.e. dioxygen complexes, peroxides, and metal dioxides [2,25,26]. Even in the case of a simple metal cluster such as [Fe_2, O_2] the possibilities are daunting, and not less than eight different structures are conceivable for the neutral species [14]. Further, as suggested by theoretical studies [27], we may neglect thermal corrections to reaction enthalpies for the ICR experiments performed at 298 K, and refer to 0 K values throughout.

3.1.1. Ion generation

In the gas phase, Fe_2O_2 species have so far been produced by three principally different approaches: (1) sputtering methods of bulk iron oxides or metallic iron in the presence of oxidants [6–9,11,28], (2) reactions of binuclear iron clusters with oxidants [3–8], and (3) oxidative degradation of polynuclear Fe_n^+ clusters [8,12,13]. Simply due to the possible existence of various electronic states and/or structural isomers, the different methods used for ion generation may therefore well afford certain isomers and/or states in quantities largely deviating from equilibrium populations. Further, even thermalization sequences, e.g. by way of collisions with nonreactive buffer gases, may not necessarily lead to the same populations of isomers/states when different methods for ion generation are used. This is a common limitation in the interpretation of all previous studies and also the present one insomuch the geometric and electronic nature of the $Fe_2O_2^+$ species sampled remains ambiguous. The reason for stressing this aspect right at the outset becomes obvious in the following discussion.

In this study, $Fe_2O_2^+$ is generated via approach (2), i.e. a chemical route for cluster synthesis in the gas phase. To this end, polynuclear iron carbonyl clusters are generated by association of $Fe(CO)_n^+$ ions ($n = 0$ in ICR, $n = 0$–5 in sector experiments) with neutral $Fe(CO)_5$. The $Fe_m(CO)_n^+$ clusters thus formed are subsequently reacted with dioxygen to afford the cationic iron–oxide clusters in good to moderate yields [4,5]. Under ICR conditions, the pulsed-in dioxygen can also fulfill the function of a thermalizing agent which removes excess internal energy eventually deposited in the cluster ions upon their formation.

3.1.2. Sector-field mass spectrometry

In order to characterize the $Fe_2O_2^+$ species formed by way of the chemical route for cluster synthesis in the gas phase, this cationic iron–oxide cluster is generated by CI of a mixture of $Fe(CO)_5$ and dioxygen in the CI source of a tandem mass spectrometer. After mass selection, $Fe_2O_2^+$ is subjected to various collision experiments. Collisional activation of mass-selected $Fe_2O_2^+$ affords the ionic fragments Fe_2O^+ (100%), Fe_2^+ (10%), FeO_2^+ (2%), FeO^+ (8%), and

Table 1
Thermochemical data (in kcal/mol) for $Fe_2O_2^+$ and possible fragments observed in the CA and NR mass spectra (ion masses for $^{56}Fe/^{16}O$ isotopes in amu and intensities relative to the base peak, 100%) expressed as sums of the heats of formations ($\Sigma\Delta_f H_0$) and reaction enthalpies ($\Delta_r H$) relative to the $Fe_2O_2^+$ precursor formed by CI of $Fe(CO)_5$ with O_2[a]

	Ion mass	CA	NR	$\Sigma\Delta_f H_0$[b]	$\Delta_r H$
$Fe_2O_2^+$	144	...	20	216[c]	0
$Fe_2O^+ + O$	128	100	8	315	99
$Fe_2^+ + 2O$	112	} 10	} 4	433	217
$Fe_2^+ + O_2$	112			315	99
$FeO_2^+ + Fe$	88	2	2	336	120
$FeO^+ + FeO$	72	8	50	318	102
$Fe^+ + FeO_2$	56	40	100	297	81
$O_2^+ + Fe_2$	32	<1	<1	449	233
$O^+ + Fe_2O$	16	<1	<1	461[d]	245[d]

[a] Also see [5].
[b] Derived from data given in [12], [13], and [32].
[c] Although this figure (error ± 9 kcal/mol) is derived using the most recent literature data, there is excellent agreement with an earlier prediction of $\Delta_f H_0(Fe_2O_2^+) = 215 \pm 18$ kcal/mol [3].
[d] Crude estimate using the thermochemistry of Fe_2O^+ [13] and assuming IE(Fe_2O) = 7.3 eV, i.e. the average of IE(Fe_2) = 6.2 eV [40] and IE(Fe_2O_2) = 8.4 eV (this work). IE(Fe_2O) ≪ IE(C_5H_5) = 8.41 eV [32] is further implied by the practical absence of $C_5H_5^+$ (<1%) upon collisional activation of (c-C_5H_5)Fe_2O^+ whereas the Fe_2O^+ signal is the second most intense peak (75%) in the CA spectrum of this cluster ion [38].

Fe^+ (40%); note that O_2^+ and O^+ signals are both <1%, thus disfavoring structures having intact O–O bonds for the $Fe_2O_2^+$ ion formed under these conditions [5]. Except for the formation of Fe_2O^+, which is not structurally indicative, the relative intensities of the fragments are in accord with thermochemical data available (Table 1); hence, the fragmentation pattern may, by and large, reflect energetic preferences rather than structural motifs of the incident ions. Note, however, that even though the $Fe^+ + FeO_2$ and $Fe_2^+ + O_2$ asymptotes are isoenergetic, the Fe^+ fragment is much more abundant than the Fe_2^+ channel, again disfavoring the presence of an O–O bond in $Fe_2O_2^+$.

The NR spectrum of $Fe_2O_2^+$ reveals a decent recovery signal due to reionized neutral Fe_2O_2 (20%); thus, the neutral species has a minimal lifetime in the microsecond regime. Other NR signals correspond to Fe_2O^+ (8%), Fe_2^+ (4%), FeO_2 (2%), FeO^+ (50%), and Fe^+ (100%); again, signals due to O_2^+ and O^+ are not observed above the noise level. Further, the vertical two-electron oxidation of the $Fe_2O_2^-$ anion formed upon CI in the negative ion mode was probed in an energy-resolved collision experiment [23,24]. Despite considerable error margins, these experiments can provide valuable information about the redox chemistry of transition-metal compounds [29,30]. For the CR process $Fe_2O_2^- \rightarrow Fe_2O_2^+$, an energy deficit $\Delta E_{CR} = 11.2 \pm 0.5$ eV was determined. To a first approximation, this difference is equal to the sum of the vertical detachment energy (DE_v) of the anion and the vertical ionization energy (IE_v) of the neutral species, i.e. $\Delta E_{CR} = DE_v + IE_v$. Provided that Franck-Condon effects are not too large, the relation $\Delta E_{CR} \approx EA + IE$, where EA and IE stand for the electron affinity and ionization energy of the neutral, may also hold true within the experimental error margins [30]. Neglecting differences between vertical and adiabatic transitions for the time being and using EA(Fe_2O_2) = 2.36 eV [11], we thus arrive at a first estimate of IE(Fe_2O_2) ≈ 8.8 eV ± 0.7 eV (see sec. 3.1.3.).

3.1.3. Initial reactivity studies

Although the reactivity of $Fe_2O_2^+$ under ICR conditions toward various neutrals is described in more detail further on, a few reactions relevant for the

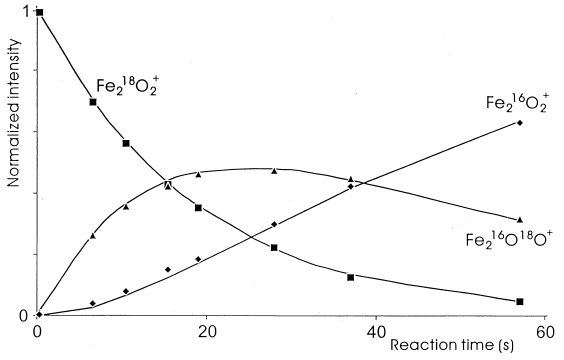

Fig. 1. Temporal product-evolution profiles in the degenerate $^{16}O/^{18}O$ exchange reactions of $Fe_2{}^{18}O_2^+$ with $H_2{}^{16}O$; symbols: $Fe_2{}^{18}O_2^+$ (square), $Fe_2{}^{16}O^{18}O^+$ (triangle), and $Fe_2{}^{16}O_2^+$ (diamond). The solid lines are derived from a kinetic fit of the consecutive reactions using $k_1/k_2 = 1.85$, see text.

characterization of the incident ion are addressed in this section already.

The first experiment to be described is $^{16}O/^{18}O$ isotopic exchange. To this end, $Fe_2{}^{18}O_2^+$ was generated by reacting mass-selected Fe^+ under ICR conditions first with pulsed-in $Fe(CO)_5$ and then with $^{18}O_2$, followed by mass selection of $Fe_2{}^{18}O_2^+$. No reactions at all occur with $^{16}O_2$, which is in keeping with the absence of an intact O–O bond in $Fe_2{}^{18}O_2^+$ for which replacement of an $^{18}O_2$ ligand in the presence of $^{16}O_2$ is expected. Instead, stepwise $^{16}O/^{18}O$ exchange is observed with water

$$Fe_2{}^{18}O_2^+ + H_2{}^{16}O \rightarrow Fe_2{}^{16}O^{18}O^+ + H_2{}^{18}O \quad (1)$$

$$Fe_2{}^{16}O^{18}O^+ + H_2{}^{16}O \rightarrow Fe_2{}^{16}O_2^+ + H_2{}^{18}O \quad (2)$$

Analysis of the reaction kinetics (Fig. 1) reveals that the ratio of the relative rate constants k_1 and k_2 is 1.85 ± 0.2, which matches the value expected for statistical $^{16}O/^{18}O$ isotope distribution ($k_1/k_2 = 2$). This observation indicates that both oxygen atoms are bound equivalently in the chemically synthesized $Fe_2O_2^+$ species described previously. However, we cannot rule out that the incoming water may catalyze O-atom equilibration [31].

Next, the IE of Fe_2O_2 is determined using the bracketing technique. To this end, mass-selected $Fe_2O_2^+$ was reacted with neutrals having well-known IEs [32] and the occurrence or absence of electron transfer from the neutral reagent to $Fe_2O_2^+$ was monitored, affording the neutral cluster concomitant with the molecular ion of the reactant. The occurrence of electron transfer close to collision rate is observed with 1,2-dihydronaphthalene (IE = 8.07 eV) and methoxybenzene (IE = 8.21 eV), whereas electron transfer is much less efficient with para-xylene (IE = 8.44 eV) and disappears with toluene (IE = 8.82 eV). Taking the reaction efficiencies into account [33], we thus estimate $IE(Fe_2O_2) = 8.4 \pm 0.3$ eV. Note that $IE(Fe_2O_2) = 8.8 \pm 0.7$ eV, derived previously from the charge-reversal experiments with $Fe_2O_2^-$, falls within the error margins of the bracketed value. This observation indicates that the structures of the anionic, neutral, and cationic species do not differ greatly, and probably all correspond to rhombic Fe_2O_2 as suggested by the matrix-isolation studies of Chertihin et al. [10] as well as theoretical predictions [14].

Finally, precisely the ion/molecule reactions studied by Gehret and Irion [8] are considered for comparison, i.e. using ammonia, benzene, and ethene as neutral substrates. Although our results for the reactions of the first two neutrals are in accordance with the previous report (see below), a dramatic difference is found for the reactivity of $Fe_2O_2^+$ toward ethene. Gehret and Irion reported exclusive occurrence of the following reaction, which these authors ascribed to a metal-cluster assisted dehydrogenation of the olefin as previously observed for other cationic transition-metal clusters [8,34]:

$$Fe_2O_2^+ + C_2H_4 \rightarrow Fe_2O_2(C_2H_2)^+ + H_2 \quad (3)$$

In contrast, reaction (3) is hardly observed in our ICR experiments as only a trace of the corresponding $Fe_2C_2H_2O_2^+$ product is formed. Although high-resolution mass analysis ($m/\Delta m \geq 100\,000$) confirms the assignment of the elemental composition of this ion, analysis of the reaction kinetics indicates that its formation is also due to secondary reactions of the initially formed products. The maximal branching ratio of the $Fe_2C_2H_2O_2^+$ channel in the $Fe_2O_2^+/C_2H_4$ couple is 2% of all primary products. Similarly, reaction with C_2D_4 yields $Fe_2C_2D_2O_2^+$ only in trace

Table 2
Summarized reactions of $Fe_2O_2^+$ with miscellaneous small neutral reagents

	Rate[a,b]	Initial products	Final products	Remarks
H_2	$<10^{-12}$			
N_2	$<10^{-12}$			
O_2	$<10^{-12}$			
N_2O	$<10^{-12}$			
CO	$<10^{-12}$			
CO_2	$<10^{-12}$			
CH_4	$<10^{-12}$			
NH_3[c]	6×10^{-10}	Fe_2ONH^+[d]	$Fe_2ONH(NH_3)^+$[c]	oxo/imino-exchange
H_2O	3×10^{-11}[e]	$Fe_2O_3H_2^+$	$Fe_2O_7H_{10}^+$	water association[f]
H_2S[g]	5×10^{-10}	Fe_2OS^+	$Fe_2S_2^+$	oxo/sulfo-exchange[h]

[a] Apparent bimolecular rate constants in cm^3 $molecules^{-1}$ s^{-1}; experimental error ± 50%.
[b] Due to clustering of $Fe_2O_2^+$ with water present in the background, rate constants $<10^{-12}$ cm^3 $molecules^{-1}$ s^{-1} cannot be observed.
[c] Also see [8].
[d] Some minor products are observed, see text.
[e] Apparent second-order rate constant at $p(H_2O) \approx 10^{-8}$ mbar; termolecular processes may be involved but are not deconvoluted.
[f] Isotopic exchange is observed upon ^{18}O labeling, see text.
[g] Also see [4].
[h] O/S exchange is also observed with COS, see [4].

amounts. Instead, various reactions occur including C–H bond activation, C–C bond cleavage, O-atom transfer, etc. Although the detailed description of the reaction products is postponed to Sec. 3.2. it needs to be pointed out at this stage that we cannot confirm the preponderance of reaction (3) in the $Fe_2O_2^+/C_2H_4$ system reported in [8]. This discrepancy of the experimental results may either be due to some instrumental shortcomings in the previous work as suggested below, or, even more significantly, different $Fe_2O_2^+$ clusters may be sampled in both experiments due to the differences in the methods used for ion generation.

3.2. Reactivity of $Fe_2O_2^+$ toward inorganic and organic substrates

Considering the severe discrepancy between the results reported in [8] and the present observations, in conjunction with the possible existence of long-lived structural and/or electronic isomers of the $Fe_2O_2^+$ cation, we refrain from an extensive description of the reactivities of the substrates, the detailed discussion of rate constants etc. Further, for those neutrals which react very efficiently with $Fe_2O_2^+$ (i.e. $k > 10^{-10}$ cm^3 $molecules^{-1}$ s^{-1}) complete thermalization of the reactant ion cannot be ensured rigorously, because at a reasonable static pressure of the neutral reagent, significant amounts of $Fe_2O_2^+$ are consumed during the time required for cluster generation. Therefore, a compromise was sought between the thermalization procedure and the signal-to-noise ratio; these rate constants and product branchings should therefore be viewed more cautiously. In regard of these ambiguities, we restrict ourselves to a phenomenological description of the reactivity of the $Fe_2O_2^+$ species formed by way of our approach in order to allow comparison with future gas-phase experiments. Further, note that, unless mentioned explicitly, the chemical formula of the ions involved, e.g. $Fe_2C_2H_2O_2^+$, only indicate the elemental composition and do not imply any particular structures.

3.2.1. Reactions with miscellaneous small molecules

Entirely consistent with [8], $Fe_2O_2^+$ does not react with several small molecules such as H_2, N_2, O_2, CO, CO_2, and N_2O at appreciable rates under ICR conditions (Table 2). With the exception of methane, reactions are observed for the element hydrides NH_3, H_2O, and H_2S which lead to the exchange of the oxo-ligands in $Fe_2O_2^+$ by imino and thio units, respectively; in the case of H_2O degenerate O-atom ex-

change occurs upon oxygen labeling (see previous discussion).

Interestingly, only one O atom in $Fe_2O_2^+$ can be replaced by an imino group in

$$Fe_2O_2^+ + NH_3 \rightarrow Fe_2ONH^+ + H_2O \quad (4a)$$

formation of $Fe_2N_2H_2^+$ according to the following reaction is not observed:

$$Fe_2ONH^+ + NH_3 \rightarrow Fe_2N_2H_2^+ + H_2O \quad (4b)$$

In contrast, both O atom are easily exchanged in the case of water (as shown previously) and hydrogen sulfide [4]. These results indicate that thermochemical properties rather than kinetic barriers hamper the formation of the bisimino cluster $Fe_2N_2H_2^+$, i.e. whereas reaction (4a) is exothermic (or thermoneutral) reaction (4b) is endothermic. Considering that oxygen and sulfur are exchanged easily in combination with the fact that the oxo and imino ligands are in equilibrium in the mononuclear FeO^+/NH_3 system [35], the absence of the formal bisimino cluster $Fe_2N_2H_2^+$ suggested the operation of significant cooperative effects in the cluster.

In addition to the exchange of the oxo ligands, clustering reactions occur with the polar substrates NH_3, H_2O, and H_2S [4,8]. For example, up to five water molecules add to $Fe_2O_2^+$ to yield $Fe_2O_7H_{10}^+$, i.e. formally $Fe_2O_2(H_2O)_5^+$. Due to the low operating pressures, the ICR technique is, however, not at all ideal to study the details of such association reactions and much higher degrees of solvation are expected at elevated pressures. For example, already the bare FeO^+ cation adds up to eight water molecules in the mbar regime [36,37].

Some side reactions of the $Fe_2O_2^+/NH_3$ system are also worth mentioning, although we have not definitively clarified their genesis. Thus, in addition to Fe_2ONH^+ formed via reaction (4a), several minor products are observed at longer reaction times in the $Fe_2O_2^+/NH_3$ system. Among these is the unprecedented, and undoubtedly interesting, ion $Fe_2N_2H^+$. Since the reaction of Fe_2ONH^+ with NH_3 leading to $Fe_2N_2H^+$ requires the unlikely formation of neutral [O, H_3], additional intermediates appear to be involved. The mass-resolving power of a Fourier transform ICR (FTICR) mass spectrometer equipped with a 7.0 T magnet also permits direct observation of product ions isobaric with $Fe_2O_2^+$, such as $Fe_2ONH_2^+$ and $Fe_2(NH_2)_2^+$, and, indeed, the former ion is detected. We attribute the presence of this ion to reactions between $Fe_2O_2H^+$ and NH_3 (hydroxy-amino exchange). In turn, $Fe_2O_2H^+$ either arises from the H-atom abstraction reaction between $Fe_2O_2^+$ and NH_3 or is due to organic contaminants inevitably present as residuals in the pulse valves. In addition, we have also detected the ion Fe_2NO^+ which we believe is the precursor to $Fe_2N_2H^+$. Further, some Fe_2NO^+ is observed which may either constitute an oxo–nitrido cluster or bear an intact N–O bond [38,39]. The Fe_2NO^+ ion may be a consecutive product due to dehydrogenation of $Fe_2ONH_2^+$ or be formed in reactions between $Fe_2O_2H^+$ and NH_3 in which H_2 and H_2O are evolved.

3.2.2. Reactions with hydrocarbons

First of all, it is important to state that the $Fe_2O_2^+$ cluster is by no means unreactive as far as C–H and C–C bond activations of hydrocarbons are concerned (Table 3). Hence, the remarkable ability of the bare FeO^+ cation to activate numerous types of bonds [1,2] is not passified upon aggregation with an iron monoxide molecule. However, let us begin with the discussion of the $Fe_2O_2^+/C_2H_4$ couple in more detail, because it is this particular system which gives rise to the severe discrepancies in the comparison with the data reported in [8]. The reactions of some other hydrocarbons are then addressed more briefly further below.

As mentioned previously, Gehret and Irion reported the exclusive occurrence of reaction (3) for the $Fe_2O_2^+/C_2H_4$ couple [8]. In our experiments, a variety of products in the following reactions are observed and the corresponding dehydrogenation channel leading to $Fe_2C_2H_2O_2^+$ constitutes a very minor one:

$$Fe_2O_2^+ + C_2H_4 \rightarrow Fe_2O^+ + C_2H_4O \quad 5\% \quad (5a)$$

$$\rightarrow Fe_2OH_2^+ + C_2H_2O \quad 5\% \quad (5b)$$

$$\rightarrow Fe_2CH_4O^+ + CO \quad 25\% \quad (5c)$$

Table 3
Summarized reactions of $Fe_2O_2^+$ with selected hydrocarbons

	Rate[a,b]	Primary products (branching)
CH_4	$<10^{-12}$	
C_2H_6	$<10^{-12}$	
C_3H_8	5×10^{-12}[c,d]	$Fe_2O_2H_2^+$ (80), $Fe_2O_2(C_3H_8)^+$ (20)
n-C_4H_{10}	3×10^{-11}[c]	$C_4H_9^+$ (7), $Fe_2O_2H_2^+$ (55), $Fe_2C_2H_6O_2^+$ (5), $Fe_2C_4H_8O^+$ (5), $Fe_2O_2(C_4H_{10})^+$ (28)
c-C_3H_6	4×10^{-10}	$Fe_2O_2H^+$ (15), $Fe_2O_2H_2^+$ (15), $Fe_2C_3H_4O_2^+$ (70)
c-C_6H_{12}	2×10^{-10}	$C_6H_{11}^+$ (20), $FeC_6H_6^+$ (5), $Fe_2O_2H_2^+$ (15), $Fe_2C_6H_8O_2^+$ (60)
C_2H_4[e]	3×10^{-10}	Fe_2O^+ (5), $Fe_2OH_2^+$ (5), $Fe_2CH_4O^+$ (25), $Fe_2O_2H_2^+$ (40), $Fe_2C_2H_2O^+$ (15), $Fe_2CO_2^+$ (8), $Fe_2C_2H_2O_2^+$ (2)[f]
Z-C_4H_8	7×10^{-10}	Fe^+ (5), $FeC_4H_6^+$ (5), $Fe_2O_2H_2^+$ (45), $Fe_2C_4H_6O^+$ (45)
i-C_4H_8	8×10^{-10}	$Fe_2OH_2^+$ (10), $Fe_2O_2H_2^+$ (10), $Fe_2C_3H_4O^+$ (10), $Fe_2C_3H_6O^+$ (15), $Fe_2C_4H_6O^+$ (55)
c-C_6H_6	4×10^{-10}[c,g]	$Fe_2O_2(C_6H_6)^+$ (100)

[a] Apparent bimolecular rate constant in cm^3 $molecules^{-1}$ s^{-1}; experimental error ±50%.
[b] Due to clustering of $Fe_2O_2^+$ with water present in the background, rate constants $<10^{-12}$ cm^3 $molecules^{-1}$ s^{-1} cannot be observed.
[c] Apparent second order rate constants at ~10^{-8} mbar; termolecular processes may be involved in the formations of the formal adduct complexes $Fe_2O_2(C_3H_8)^+$, $Fe_2O_2(C_4H_{10})^+$, and $Fe_2O_2(C_6H_6)^+$ for propane, butane, and benzene, respectively, but are not deconvoluted.
[d] Minor amounts (<2%) of $C_3H_7^+$ cation are observed.
[e] Product branching for the $Fe_2O_2^+/C_2D_4$ couple: Fe_2O^+ (7), $Fe_2OD_2^+$ (4), $Fe_2CD_4O^+$ (20), $Fe_2O_2D_2^+$ (35), $Fe_2CO_2^+$ (10), $Fe_2C_2D_2O^+$ (20), $Fe_2C_2D_2O_2^+$ (2), $Fe_2O_2(C_2D_4)^+$ (2).
[f] A trace amount (~1%) of the formal adduct complex $Fe_2O_2(C_2H_4)^+$ is observed, but it may be due to secondary reactions of the initial products.
[g] A rate constant of 1.5×10^{-10} cm^3 $molecules^{-1}$ s^{-1} is given in [8]; no pressure mentioned.

$$\rightarrow Fe_2O_2H_2^+ + C_2H_2 \quad 40\% \quad (5d)$$

$$\rightarrow Fe_2C_2H_2O^+ + H_2O \quad 15\% \quad (5e)$$

$$\rightarrow Fe_2CO_2^+ + CH_4 \quad 8\% \quad (5f)$$

$$\rightarrow Fe_2C_2H_2O_2^+ + H_2 \quad 2\% \quad (5g)$$

We deliberately avoid specification of a product structure for reaction (5e).

First of all, it is worth mentioning that several different types of reactions are observed ranging from O-atom transfers in reactions (5a) and (5b) to reductive and oxidative dehydrogenations [reactions (5d), (5e), and (5g)] and C–C bond cleavages in reactions (5c) and (5f). As far as thermochemical data are concerned, useful information can only be derived for reaction (5a) which is exothermic if either acetaldehyde or CH_4 + CO are the neutral products, i.e. $\Delta_r H(5a) = -11$ and -17 kcal/mol, respectively; the reaction is endothermic by 16 kcal/mol if oxirane were formed [32]. Occurrence of reaction (5d) for the thermalized ions further implies that the sum $D(Fe_2O_2^+ - H) + D(Fe_2O_2H^+ - H) \geq 144$ kcal/mol [32]. Conclusive thermochemical analysis of all other channels fails due to the limited number of appropriate reference data for ligated Fe_m^+ clusters [12,13,34,40].

A possible rationale for the dramatic difference between our results and those reported in [8] can be derived from the fact that the $Fe_2CH_4O^+$ product ion formed in reaction (5c) is nominally isobaric to the $Fe_2O_2^+$ reactant (both 144 u); nevertheless, the ions are completely mass-resolved in the FTICR experiments ($m/\Delta m > 100\,000$). In their preliminary report on the chemistry of the micro-oxides of iron, Gehret and Irion have not mentioned this particular anomaly. Hence, it could be possible that the differences observed are due to mass-selection of mixtures of $Fe_2CH_4O^+$ and $Fe_2O_2^+$. Although this scenario would pleasingly explain the discrepancies, if $Fe_2C_2H_2O_2^+$ were a secondary product of $Fe_2CH_4O^+$, kinetic analysis of the consecutive reactions of $Fe_2CH_4O^+$ provides no evidence for the formation of $Fe_2C_2H_2O_2^+$. Instead the major route for the depletion of the $Fe_2CH_4O^+$ ion is reaction with water present in the background of the instrument by way of

$$Fe_2CH_4O^+ + H_2O \rightarrow Fe_2O_2H_2^+ + CH_4 \quad (6)$$

Hence, we simply cannot provide any reasonable explanation for the results of Gehret and Irion [8] other than their experiments sampled different $Fe_2O_2^+$ species than ours. Within this context, it is also noteworthy that the occurrence of the following reactions was reported in [8], implying $D_0(Fe_2O^+–O) \geq 127$ and 118 kcal/mol, respectively:

$$Fe_2O^+ + CO_2 \rightarrow Fe_2O_2^+ + CO \quad (7)$$

$$Fe_2O^+ + O_2 \rightarrow Fe_2O_2^+ + O \quad (8)$$

This result neither is consistent with the recently determined value $D_0(Fe_2O^+–O) = 99.2 \pm 7.7$ kcal/mol [12] nor agrees with the oxygen-atom transfer from $Fe_2O_2^+$ to ethene observed in reaction (5a) which can only concur with thermalized ions if $D_0(Fe_2O^+ - O) \leq 111$ kcal/mol [32]. Note, however, that one cannot necessarily conclude that the experiments of Gehret and Irion [8] involved "hot" ions because the formation of different isomers and/or states of $Fe_2O_2^+$ in the various modes used for cluster-ion generation could account for these discrepancies as well [4–9,11–13]. In fact, if the experiments by Gehret and Irion were considered to truly correspond to reactions of thermalized ions, the reported occurrence of reactions (7) and (8) implies the formation of a more stable $Fe_2O_2^+$ structure than that sampled by Griffin and Armentrout [12,13] as well as reported in this work.

In order to validate our analysis and shed further light on the reaction products, the reaction of $Fe_2O_2^+$ with C_2D_4 is considered. Experimentally, the same, but deuterated products are observed with by and large similar branching ratios (see footnote e in Table 3); the only exception is the notable amount of the formal adduct complex $Fe_2O_2(C_2D_4)^+$ which is hardly observed in the unlabeled system. Structurally indicative are the consecutive H/D exchange reactions observed with water present in the background as well as other secondary processes (Table 4). The Fe_2O^+ ion undergoes clustering with water and ethene to afford the corresponding adducts. No H/D-exchange of $Fe_2OD_2^+$ is observed, and instead the disappearance of this primary product ion is attributed to the formation of $Fe_2O_2HD^+$ and $Fe_2O_2H_2^+$. Also interesting is

Table 4
Secondary reactions of the products of the $Fe_2O_2^+/C_2D_4$ couple with C_2D_4 and water present in the background

	Secondary products[a,b]
Fe_2O^+	$Fe_2O_2H_2^+$, $Fe_2O(C_2D_4)^+$
$Fe_2OD_2^+$	$Fe_2O_2HD^+$, $Fe_2O_2H_2^+$
$Fe_2CD_4O^+$	$Fe_2O_2HD^+$, $Fe_2O_2H_2^+$
$Fe_2O_2D_2^+$	$Fe_2O_2HD^+$, $Fe_2O_2H_2^+$, $Fe_2O_3H_4^+$, $Fe_2O_2H_2(C_2D_4)^+$
$Fe_2C_2D_2O^+$	$Fe_2C_2HDO^+$, $Fe_2C_2H_2O^+$
$Fe_2CO_2^+$	$Fe_2O_2H_2^+$, $Fe_2O(C_2D_4)^+$
$Fe_2C_2D_2O_2^+$	$Fe_2C_2D_2O_2^+$
$Fe_2O_2(C_2D_4)^+$	$Fe_2O_2(C_2HD_3)^+$, $Fe_2O_2(C_2H_2D_2)^+$, $Fe_2O_2(C_2H_3D)^{+c}$

[a] Derived from the analysis of the reaction kinetics of the $Fe_2O_2^+/C_2D_4$ couple with water present in the background also.
[b] Elemental compositions of all products are confirmed by high-resolution mass measurements.
[c] $Fe_2O_2(C_2H_4)^+$ is not detected, but appears likely to be formed at longer reaction times.

that neither clustering with C_2D_4 nor H/D exchanges with water occur with $Fe_2CD_4O^+$, and the reaction kinetics again imply formation of $Fe_2O_2HD^+$ and $Fe_2O_2H_2^+$ as major secondary products. Instead, $Fe_2O_2D_2^+$ undergoes very rapid H/D exchange with water to afford $Fe_2O_2HD^+$ and $Fe_2O_2H_2^+$; at longer reaction times, this ion undergoes clustering with water and ethene to yield $Fe_2O_3H_4^+$ and $Fe_2O_2H_2(C_2D_4)^+$, respectively. For the $Fe_2C_2D_2O^+$ and $Fe_2C_2D_2O_2^+$ species, up to two H/D exchanges are observed to yield the corresponding unlabeled ions. In addition, the formal adduct $Fe_2O_2(C_2D_4)^+$ undergoes sequential H/D exchange. Secondary reactions of the minor $Fe_2CO_2^+$ product lead to $Fe_2O_2H_2^+$ and $Fe_2O(C_2D_4)^+$, i.e. exchange of a carbonyl ligand by water and ethene, respectively. Interestingly, trace amounts of $Fe_2O_3^+$ are also detected which are attributed to the previously suggested formation of this species by exchange of a CO ligand in $Fe_2CO_2^+$ by molecular oxygen which is also present in the background [5]. These results are consistent with the structural suggestions displayed in Scheme 1 for the reactions of $Fe_2OD_2^+$, $Fe_2CD_4O^+$, and $Fe_2O_2D_2^+$ product ions with water. Here, it is assumed that all clusters share one bridging hydroxy ligand while the second bridge consists of a hydrido ligand in $Fe_2OD_2^+$, a methyl ligand in $Fe_2CD_4O^+$, and a further

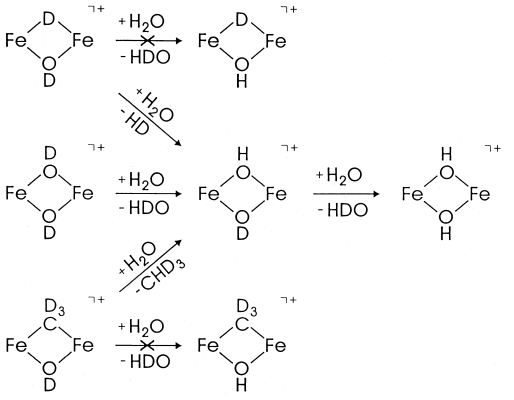

Scheme 1.

hydroxy group in $Fe_2O_2D_2^+$; similarly, the $Fe_2CO_2^+$ ion can be regarded as an Fe_2O^+ unit with a bridging carbonyl ligand. It needs to be stressed, however, that these structures are no more than educated guesses because no detailed information on the structural properties of ligated iron clusters is available so far. For example, whether or not the structures bear the proposed formal C_s symmetries, whether or not there exist Fe–Fe bonds etc. is entirely unknown. Concerning the sequential H/D exchanges of the other products, i.e. $Fe_2C_2D_2O^+$, $Fe_2C_2D_2O_2^+$, as well as the formal adduct $Fe_2O_2(C_2D_4)^+$, not even tentative structural proposals are possible for the time being.

Based on these results, a mechanistic scenario is suggested for the $Fe_2O_2^+/C_2H_4$ couple (Scheme 2) in which we deliberately do not include any structural inferences. With regard to the product distribution it is

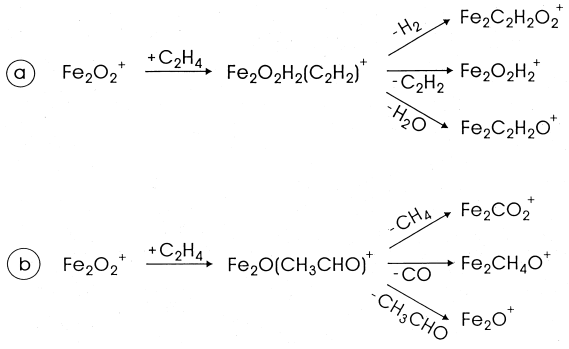

Scheme 2.

obvious that at least two different mechanisms must be operative, i.e. route (a) in which C–H bond activation predominates in the first step leading to reactions (5d), (5e), and (5g), and route (b) which involves O-atom transfer to the carbon skeleton and in which formation of acetaldehyde as an intermediate can account for reactions (5a), (5c), and (5f). The generation of the $Fe_2OH_2^+$ ion concomitant with expulsion of ketene in reaction (5b) can occur by means of either of these or even a third route. Involvement of acetaldehyde as a conceivable reaction intermediate is based upon analogies from the chemistry of mononuclear metal oxides with ethene. For example, formation of acetaldehyde as the neutral product of O-atom transfer to ethene from CrO^+ [41], FeO^+ [42], and VO_2^+ [43], respectively, has been inferred. Note, however, that the nature of the neutral(s) remain unknown in these ICR experiments, and with regard to the product distribution in reaction (5) as well as the favorable thermochemistry, $CH_4 + CO$ could also be formed, i.e. $\Delta_f H_0(CH_3CHO) = -37$ kcal/mol versus $\Sigma\Delta_f H_0(CH_4 + CO) = -43$ kcal/mol.

After having extensively discussed the ethene case, the reactions of $Fe_2O_2^+$ with some other hydrocarbons are briefly addressed (Table 3). Methane and ethane do not react at measurable rates and also the activations of propane and *n*-butane proceed slowly, with C–H bond activations predominating, though some C–C bond cleavage is also observed in the case of *n*-butane. The small rate constants are consistent with significant amounts of the formal adducts observed for these alkanes. Notable are the carbocation formations corresponding to formal hydride transfers from the alkanes to the iron–oxide cluster (see the following). Compared to the aliphatic hydrocarbons, the two cycloalkanes examined are more reactive by about an order of magnitude. Again, C–H bond activations predominate. Consistent with the larger rate constants for these substrates, formation of the formal adducts is not observed anymore. Quite interesting is the formation of the mononuclear $FeC_6H_6^+$ cluster from the $Fe_2O_2^+/c\text{-}C_6H_{12}$ couple because it is an example for cluster degradation coupled with multiple dehydrogenation according to reaction (9):

$$Fe_2O_2^+ + c\text{-}C_6H_{12} \rightarrow FeC_6H_6^+ + Fe(OH)_2 + 2H_2 \quad (9)$$

Reaction (9) is among the few processes for which further thermochemical considerations can be pursued. Multiple dehydrogenation of cyclohexane by transition-metal cations is quite common [44], and thus we may assume that the $FeC_6H_6^+$ product corresponds to iron cation ligated by benzene with $D(Fe^+ - C_6H_6) = 49.6 \pm 2.3$ kcal/mol [45]. Using $\Delta_f H_0(Fe(OH)_2) = -77 \pm 5$ kcal/mol [27], reaction (9) is thus predicted to be exothermic by about 17 kcal/mol. Observation of Fe–Fe bond rupture in reaction (9) is therefore consistent with the notion of monitoring thermalized $Fe_2O_2^+$ ions under our conditions. Cyclopropane is the only hydrocarbon which also gives rise to the formation of open-shell neutrals upon reaction with $Fe_2O_2^+$, i.e. $C_3H_5^{\cdot}$ is formed concomitant with $Fe_2O_2H^+$; the latter ion continues to react with *c*-C_3H_6 to afford $Fe_2O_2H_2^+$ by means of a second H-atom abstraction from cyclopropane. With the reasonable assumption that allyl radical *l*-$C_3H_5^{\cdot}$ rather than cyclopropyl radical *c*-$C_3H_5^{\cdot}$ is formed as a neutral, we can derive the lower limits $D(Fe_2O_2^+–H) \geq 78$ kcal/mol and $D(Fe_2O_2H^+–H) \geq 78$ kcal/mol from the literature thermochemistry of the following reaction [32,46]:

$$c\text{-}C_3H_6 \rightarrow l\text{-}C_3H_5^{\cdot} + H^{\cdot} \qquad \Delta_r H = 78 \text{ kcal/mol} \quad (10)$$

these figures agree with the lower bound of ≥144 kcal/mol derived above for their sum.

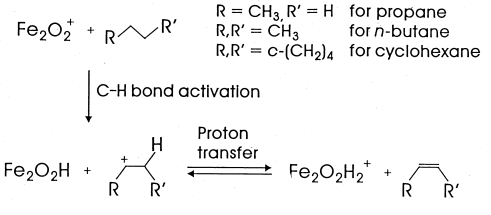

Scheme 3.

Let us briefly return to the carbocation formation in the reactions of $Fe_2O_2^+$ with alkanes. This channel is connected to the $Fe_2O_2H_2^+$ product by simple proton transfer (Scheme 3). If we assume that the ratio between the carbocation products and $Fe_2O_2H_2^+$ is governed by thermochemical properties rather than kinetic phenomena, the ratios $C_3H_7^+/Fe_2O_2H_2^+ < 0.025$ for propane, $C_4H_9^+/Fe_2O_2H_2^+ \approx 0.125$ for *n*-butane, and $C_6H_{11}^+/Fe_2O_2H_2^+ \approx 1.33$ for cyclohexane imply that the proton affinity (PA) of neutral Fe_2O_2H exceeds those of propene (PA = 179.6 kcal/mol [47]) and butene (PA = 179.5 kcal/mol for *Z*-2-butene [32,47]), but is smaller than that of cyclohexene (PA = 187.4 kcal/mol [47]). Accordingly, $PA(Fe_2O_2H)$ is estimated to fall between 180 and 187 kcal/mol. However, this estimate not only assumes thermodynamic control of the proton transfer according to Scheme 3, but also relies on the absence of Wagner-Meerwein rearrangements. Thus, if *t*-$C_4H_9^+$ were formed from *n*-butane and *l*-methylcyclopentane cation, as the most stable $C_6H_{11}^+$ isomer listed in [32], from cyclohexane, the range for $PA(Fe_2O_2H)$ shifts upward to about 195 kcal/mol [47]. Further, note that the absence of carbocation formation with cyclopropane is consistent with the significantly higher ionization energy of allyl radical (IE = 8.13 eV [32]) compared to the secondary radicals *i*-$C_3H_7^{\cdot}$, *s*-$C_4H_9^{\cdot}$, and *c*-$C_6H_{11}^{\cdot}$ (IE = 7.36, 7.25, and ~6.8 eV, respectively [32]). Assuming thermodynamic control, these trends suggest $IE(Fe_2O_2H)$ to lie between 7.3 and 8.1 eV and 180 kcal/mol < $PA(Fe_2O_2H)$ < 195 kcal/mol.

Quite remarkable are the pronounced differences in the product distributions for *Z*- and iso-butene because this rules out complete loss of structural identity of the hydrocarbon upon reaction with the $Fe_2O_2^+$ cluster. Hence, only C–H bond activation occurs with *Z*-2-butene, while significant amounts of C–C bond cleavages occur with *i*-butene. A straightforward rationale for the difference is that C–H bond activations of linear butenes allow formation of a conjugated diene, whereas this option is blocked for the branched skeleton [48]. Hence, twofold allylic C–H bond activation of *Z*-2-butene can afford a butadiene complex which can then either eliminate water, butadiene, or neutral $Fe(OH)_2$ to afford $Fe_2C_4H_6O^+$, $Fe_2O_2H_2^+$, and $FeC_4H_6^+$, respectively; again, Fe–Fe scission in the following reaction is consistent with thermochemical data which predict an

exothermicity of ~28 kcal/mol when butadiene/Fe^+ is formed as ionic product [32,49]:

$$Fe_2O_2^+ + Z\text{-}C_4H_8 \rightarrow FeC_4H_6^+ + Fe(OH)_2 \qquad (11)$$

Finally, the association of $Fe_2O_2^+$ with benzene agrees with the results given in [6]; the difference in the apparent bimolecular rate constants should not be overrated, because associations with benzene are likely to involve termolecular contributions. At longer reaction times, $Fe_2O_2(C_6H_6)^+$ continues to react with benzene as well as background water to afford the formal bisadducts $Fe_2O_2(C_6H_6)_2^+$ and $Fe_2O_2(C_6H_6)(H_2O)^+$, respectively, of which the former predominates at long reaction times.

4. Conclusions

The cationic iron–oxide cluster $Fe_2O_2^+$ exhibits a rich reactivity toward various substrates which differ considerably from that of mononuclear metal-oxide cations for which C–H bond activation occurs almost exclusively [1,2]. Although C–H bond activations also predominate in the reactions of $Fe_2O_2^+$ with hydrocarbons, C–C bond cleavages, O-atom transfers from the metal oxide to the substrates, and even Fe–Fe ruptures are observed to some extent. Although these reactions shed light on the properties of metal-oxide clusters as models for oxidation catalysts based on these materials, the most important observation at this stage is the dramatic difference between the present results and those reported in [8] for the $Fe_2O_2^+$/ethene couple. A possible explanation is that the different methods used in these studies for the generation of the cluster ions do not lead to identical populations of isomers and/or states in both experimental studies. This observation is of major significance for the evaluation of cluster-ion reactivities, insomuch as the existence of structural and/or electronic isomers deserves more careful scrutiny. Further studies of this interesting aspect in the gas-phase ion chemistry of $Fe_2O_2^+$ are indicated. Particularly valuable would be techniques which probe the relationships between the clusters' generation and their specific reactivities.

Finally, if it is assumed that the present as well as previous experiments referred to the respective $Fe_2O_2^{+/0/-}$ species in their most stable forms, the previously determined values $D_0(Fe^+–Fe) = 64.1 \pm 2.1$ kcal/mol [40], $D_0(Fe_2O^+ - O) = 99.2 \pm 7.7$ kcal/mol [12,13], $D_0(Fe_2^+–O) = 117.6 \pm 4.6$ kcal/mol [13], and $EA(Fe_2O_2) = 2.36$ eV in conjunction with $IE(Fe_2O_2) = 8.4 \pm 0.3$ eV determined in this work suggest heats of formation of $\Delta_f H_0(Fe_2O_2^-) = -32 \pm 12$ kcal/mol, $\Delta_f H_0(Fe_2O_2) = 22 \pm 12$ kcal/mol, and $\Delta_f H_0(Fe_2O_2^+) = 216 \pm 9$ kcal/mol for the anionic, neutral, and cationic di-iron dioxide. Further, the ion/molecule reactions observed here provide lower limits for the bond strengths $D_0(Fe_2O_2^+–H) \geq 78$ kcal/mol, $D_0(Fe_2O_2^+–H) \geq 78$ kcal/mol, and $D_0(Fe_2O_2^+–H) + D_0(Fe_2O_2^+–H) \geq 144$ kcal/mol, respectively, as well as the estimates $IE(Fe_2O_2H) \approx 7.3–8.4$ eV and $PA(Fe_2O_2H) \approx 180–195$ kcal/mol.

Acknowledgements

The authors thank the Deutsche Forschungsgemeinschaft, the Volkswagen-Stiftung, and the Fonds der Chemischen Industrie for continuous financial support. P.B. Armentrout is acknowledged for helpful discussions concerning the thermochemistry of $Fe_2O_2^+$ reported in [12] and [13]. One of the authors (J.N.H.) thanks the Alexander von Humboldt-Stiftung for a research fellowship.

References

[1] D. Schröder, H. Schwarz, Angew. Chem. 107 (1995) 2126; Angew. Chem. Int. Ed. Engl. 34 (1995) 1973.
[2] D. Schröder, S. Shaik, H. Schwarz, Structure and Bonding, B. Meunier (Ed.), Springer, Berlin, 97 (2000) 91.
[3] D.B. Jacobson, B.S. Freiser, J. Am. Chem. Soc. 108 (1986) 27.
[4] J.N. Harvey, D. Schröder, H. Schwarz, Inorg. Chim. Acta 273 (1998) 111.
[5] D. Schröder, P. Jackson, H. Schwarz, Eur. J. Inorg. Chem., (2000) 1171.
[6] S.J. Riley, E.K. Parks, G.C. Nieman, L.G. Pobo, S. Wexler, J. Chem. Phys. 80 (1984) 1360.
[7] R.L. Whetten, D.M. Cox, D.J. Trevor, A. Kaldor, J. Phys. Chem. 89 (1985) 566.

[8] O. Gehret, M.P. Irion, Eur. J. Chem. 2 (1996) 598.
[9] M.C. Oliveira, J. Marcalo, M.C. Viera, M.A. Almoster Ferreira, Int. J. Mass Spectrom. 185/186/187 (1999) 825.
[10] G.V. Chertihin, W. Saffel, J.T. Yustein, M. Neurock, A. Ricca, C.W. Bauschlicher Jr., L. Andrews, J. Phys. Chem. 100 (1996) 5261.
[11] H. Wu, S.R. Desai, L.-S. Wang, J. Am. Chem. Soc. 118 (1996) 5296.
[12] J.B. Griffin, P.B. Armentrout, J. Chem. Phys. 106 (1997) 4448.
[13] J.B. Griffin, P.B. Armentrout, J. Chem. Phys. 107 (1997) 5345.
[14] Z. Cao, M. Duran, M. Solà, J. Chem. Soc. Faraday Trans. 94 (1998) 2877.
[15] K. Eller, H. Schwarz, Int. J. Mass Spectrom. Ion Processes 93 (1989) 243.
[16] K. Eller, W. Zummack, H. Schwarz, J. Am. Chem. Soc. 112 (1990) 621.
[17] R.A. Forbes, F.H. Laukien, J. Wronka, Int. J. Mass Spectrom. Ion Processes 83 (1988) 23.
[18] D. Schröder, H. Schwarz, D.E. Clemmer, Y.-M. Chen, P.B. Armentrout, V.I. Baranov, D.K. Böhme, Int. J. Mass Spectrom. Ion Processes 161 (1997) 177.
[19] C.A. Schalley, D. Schröder, H. Schwarz, Int. J. Mass Spectrom. Ion Processes 153 (1996) 173.
[20] J.L. Holmes, Org. Mass Spectrom. 20 (1985) 169.
[21] N. Goldberg, H. Schwarz, Acc. Chem. Res. 27 (1994) 347.
[22] M.M. Bursey, Mass Spectrom. Rev. 9 (1990) 555.
[23] J.N. Harvey, D. Schröder, H. Schwarz, Bull. Soc. Chim. Belg. 106 (1997) 447.
[24] D. Schröder, J.N. Harvey, M. Aschi, H. Schwarz, J. Chem. Phys. 108 (1998) 8446.
[25] D. Schröder, A. Fiedler, W. A. Herrmann, H. Schwarz, Angew. Chem. 107 (1995) 2714; Angew. Chem. Int. Ed. Engl. 34 (1995) 2517.
[26] D. Schröder, H. Schwarz, Helv. Chim. Acta, in press.
[27] C.B. Kellogg, K.K. Irikura, J. Phys. Chem. A 103 (1999) 1150.
[28] B. Maunit, A. Hachimi, P. Manuelli, P.J. Calba, J.F. Muller, Chem. Phys. Lett. 156 (1996) 173.
[29] J.N. Harvey, C. Heinemann, A. Fiedler, D. Schröder, H. Schwarz, Chem. Eur. J. 2 (1996) 1230.
[30] D. Schröder, S. Bärsch, H. Schwarz, Int. J. Mass Spectrom. 192 (1999) 125.
[31] H. Becker, D. Schröder, W. Zummack, H. Schwarz, J. Am. Chem. Soc. 116 (1994) 1096.
[32] S.G. Lias, J.E. Bartmess, J.F. Liebman, J.L. Holmes, R.D. Levin, W.G. Mallard, J. Phys. Chem. Ref. Data 17 (1988), Suppl. 1.
[33] G. Bouchoux, J.Y. Salpin, D. Leblanc, Int. J. Mass Spectrom. Ion Processes 153 (1996) 37.
[34] P. Schnabel, M.P. Irion, Ber. Bunsenges. Phys. Chem. 96 (1992) 1101, and references cited therein.
[35] M. Brönstrup, I. Kretzschmar, D. Schröder, H. Schwarz, Helv. Chim. Acta 81 (1998) 2348.
[36] V. Baranov, G. Javahery, A.C. Hopkinson, D.K. Bohme, J. Am. Chem. Soc. 117 (1995) 12801.
[37] P. Pradel, L. Poisson, J.M. Mestdagh, C. Rolando, J. Chem. Soc. Faraday Trans. 93 (1997) 1697.
[38] J.J. Klaassen, D.B. Jacobsen, J. Am. Chem. Soc 110 (1988) 974.
[39] D. Schröder, J. Müller, H. Schwarz, Organometallics 12 (1993) 1972.
[40] P.B. Armentrout, B.L. Kickel, Organometallic Ion Chemistry, B.S. Freiser (Ed.), Kluwer, Dordrecht, 1996, p. 1.
[41] H. Kang, J.L. Beauchamp, J. Am. Chem. Soc. 108 (1986) 5663.
[42] D. Schröder, H. Schwarz, Angew. Chem. 102 (1990) 1466; Angew. Chem. Int. Ed. Engl. 29 (1990) 1431.
[43] J.N. Harvey, M. Diefenbach, D. Schröder, H. Schwarz, Int. J. Mass Spectrom. 182/183 (1999) 85.
[44] K. Seemeyer, D. Schröder, M. Kempf, O. Lettau, J. Müller, H. Schwarz, Organometallics 14 (1995) 4465, and references cited therein.
[45] F. Meyer, F.A. Khan, P.B. Armentrout, J. Am. Chem. Soc. 117 (1995) 9740.
[46] J. Berkowitz, G.B. Ellison, D. Gutman, J. Phys. Chem. 98 (1994) 2744.
[47] E.P.L. Hunter, S.G. Lias, J. Phys. Chem. Ref. Data 27 (1998) 413.
[48] R. Wesendrup, C.A. Schalley, D. Schröder, H. Schwarz, Organometallics 15 (1996) 1435, and references cited therein.
[49] D. Schröder, H. Schwarz, J. Organomet. Chem. 504 (1995) 123.